


Chemosensitive Phox2b-expressing neurons are crucial for hypercapnic ventilatory response in the nucleus tractus solitarius

Congrui Fu^{1,*}, Jinyu Xue^{2,*}, Ri Wang¹, Jinting Chen¹, Lan Ma¹, Yixian Liu¹, Xuejiao Wang¹, Fang Guo³, Yi Zhang¹, Xiangjian Zhang^{4,5} and Sheng Wang^{1,5} 

¹Department of Physiology, Hebei Medical University, Shijiazhuang, Hebei, China

²Department of Respiration, Hebei Chest Hospital, Shijiazhuang, Hebei, China

³Department of Pharmacology, Hebei Medical University, Shijiazhuang, Hebei, China

⁴Department of Neurology, Second Hospital of Hebei Medical University, Shijiazhuang, Hebei, China

⁵Hebei Key Laboratory of Vascular Homeostasis and Hebei Collaborative Innovation Center for Cardio-cerebrovascular Disease, Shijiazhuang, Hebei, China

Key points

- Central hypercapnic hypoventilation is highly prevalent in children suffering from congenital central hypoventilation syndrome (CCHS).
- Mutations of the gene for paired-like homeobox 2b (Phox2b) are aetiologically associated with CCHS and Phox2b is present in central components of respiratory chemoreflex, such as the nucleus tractus solitarius (NTS).
- Injection of the neurotoxin substance P-saporin into NTS destroys Phox2b-expressing neurons. Impaired hypercapnic ventilatory response caused by this neurotoxin is attributable to a loss of CO₂-sensitive Phox2b-expressing NTS neurons.
- A subgroup of Phox2b-expressing neurons exhibits intrinsic chemosensitivity. A background K⁺ channel-like current is partially responsible for such chemosensitivity in Phox2b-expressing neurons.
- The present study helps us better understand the mechanism of respiratory deficits in CCHS and potentially locates a brainstem site for development of precise clinical intervention.

Abstract The nucleus tractus solitarius (NTS) neurons have been considered to function as central respiratory chemoreceptors. However, the common molecular marker defined for these neurons remains unknown. The present study investigated whether paired-like homeobox 2b (Phox2b)-expressing NTS neurons are recruited in hypercapnic ventilatory response (HCVR) and whether these neurons exhibit intrinsic chemosensitivity. HCVR was assessed using whole body plethysmography and neuronal chemosensitivity was examined by patch clamp recordings in brainstem slices or dissociated neurons from Phox2b-EGFP transgenic mice. Injection of the neurotoxin substance P-saporin (SSP-SAP) into NTS destroyed Phox2b-expressing neurons. Minute ventilation and tidal volume were both reduced by 13% during exposure to 8% CO₂ in inspired air when ~13% of the Phox2b-expressing neurons were eliminated. However, a loss of ~18% of these neurons was associated with considerable decreases in minute ventilation by ≥18% and in tidal volume by ≥22% when challenged by ≥4% CO₂. In both cases, breathing frequency was unaffected. Most CO₂-activated neurons were immunoreactive to Phox2b. In brainstem slices, ~43% of Phox2b-expressing neurons from Phox2b-EGFP mice displayed a sustained or transient

*These authors contributed equally to this work.

increase in firing rate during physiological acidification (pH 7.0 or 8% CO₂). Such a response was also present in dissociated neurons in favour of an intrinsic property. In voltage clamp recordings, a background K⁺ channel-like current was found in a subgroup of Phox2b-expressing neurons. Thus, the respiratory deficits caused by injection of SSP-SAP into the NTS are attributable to proportional lesions of CO₂/H⁺-sensitive Phox2b-expressing neurons.

(Resubmitted 4 April 2017; accepted after revision 4 May 2017; first published online 10 May 2017)

Corresponding author S. Wang: Department of Physiology, Hebei Medical University, 361 East Zhongshan Road, Shijiazhuang, Hebei 050017, China. Email: wangsheng@hebmu.edu.cn

Abbreviations AP, area postrema; ASIC, acid sensitive ion channel; CCHS, congenital central hypoventilation syndrome; DMNV, dorsal motor nucleus of vagus; HCVR, hypercapnic ventilatory response; NK1R, neurokinin-1 receptor; NeuN, neuronal nuclear antigen; NTS, nucleus tractus solitarius; Phox2b, paired-like homeobox 2b; RTN, retrotrapezoid nucleus; SSP-SAP, substance P-saporin; WBP, whole body plethysmography.

Introduction

The central respiratory chemoreflex maintains acid–base balance by regulation of pulmonary ventilation, and is therefore one of the essential homeostatic mechanisms. Structural and functional deficiency of central respiratory chemoreceptors will result in impaired hypercapnic ventilatory response (HCVR); for example, in congenital central hypoventilation syndrome (CCHS) and central sleep apnoea (Weese-Mayer *et al.* 2010). CCHS, with clinical signs of an absence of HCVR during sleep, is presumably caused by mutations of the gene for paired-like homeobox 2b (Phox2b), which is expressed in the central components of the respiratory chemoreflex (Dubreuil *et al.* 2009a; Goridis *et al.* 2010), consisting of nucleus tractus solitarius (NTS) and retrotrapezoid nucleus (RTN). Phox2b is required for the development of most neurons in the NTS and persists into adulthood in the NTS (Dauger *et al.* 2003; Stornetta *et al.* 2006; Kang *et al.* 2007).

The regulation of pulmonary ventilation by NTS neurons has been well established in *in vivo* experiments (Dean & Putnam, 2010). According to these studies, focal lesioning and pharmacological blockade of a portion of the NTS region attenuated HCVR. For example, injection of kainic acid into the ventrolateral subnucleus of the NTS in anaesthetized rats decreased significantly HCVR (Berger & Cooney, 1982), followed by the experiments demonstrating that a large NTS region (but not limited to the ventrolateral region) contributed to regulation of HCVR (Nattie & Li, 2002a; Nattie & Li, 2008). In addition, chemosensitive neurons were found in various subnuclei of the NTS using *in vitro* slices or dissociated neurons (Dean *et al.* 2001; Nichols *et al.* 2008; Huda *et al.* 2012). Nevertheless, the molecular signature of NTS neurons as candidate central respiratory chemoreceptors remains undefined. Accordingly, determining whether Phox2b-expressing NTS neurons as a putatively specific group contribute to HCVR could provide valuable clues with respect to a better understanding of respiratory

deficits in CCHS. Selective stimulation or lesion of Phox2b-expressing RTN neurons has been reported to trigger or blunt HCVR, respectively (Takakura *et al.* 2008; Abbott *et al.* 2009). Most Phox2b-expressing RTN neurons exhibited an intrinsic chemosensitivity, suggesting that Phox2b is a molecular signature of the chemosensitive RTN neurons (Lazarenko *et al.* 2009; Wang *et al.* 2013b). These findings are reminiscent of Phox2b-expressing NTS neurons, which may exert a similar role to RTN neurons. Considerable progress has been made towards understanding the mechanism of chemosensitive signalling. Accumulated evidence suggests the role of various chemosensitive proteins in the regulation of breathing, such as G-protein coupled receptors (Kumar *et al.* 2015), transient voltage-activated K⁺ channels (Dean *et al.* 1990), acid sensitive ion channels (ASICs) (Huda *et al.* 2012) and Na⁺/HCO₃⁻ cotransport or Na⁺/Ca²⁺ exchange (Turovsky *et al.* 2016). Because the NTS is a heterogeneous nucleus, it is important to establish whether these pH-sensitive ion channels are indeed a feature of the Phox2b-expressing NTS neurons.

We therefore hypothesized that Phox2b-expressing NTS neurons are important for HCVR and that these cells possess intrinsic chemosensitivity. We utilized whole body plethysmography (WBP) to assess HCVR in conscious peripherally chemodenervated mice subjected to lesions of Phox2b-expressing NTS neurons. Furthermore, patch clamp recordings were made to investigate the chemosensitive responses of these neurons.

Methods

Animal

The *in vitro* experiments were conducted in Phox2b-EGFP-Jx101 transgenic mice generated by the GENSAT project group (The Rockefeller University, USA). The general procedures used for high-throughput bacterial artificial chromosome recombineering have been described previously (Gong *et al.* 2003). As depicted

(<http://www.informatics.jax.org/allele/MGI:4847316>), an EGFP reporter gene, followed by a polyadenylation sequence, was inserted into bacterial artificial chromosome clone RP23-15D10 at the initiating ATG codon of the first coding exon of the Phox2b gene so that EGFP expression is driven by the regulatory sequences of the BAC gene. The resulting modified BAC (BX1962) was used to generate this transgene. The *in vivo* experiments were carried out in the wild-type littermates of Jx101 transgenic mice. The genetic background of Jx101 transgenic mouse line is the mix of FVB/N and ICR mice. Mice had *ad libitum* access to water and mouse chow, and were housed individually in a controlled temperature and humidity facility under a 12:12 h light/dark cycle. All experiments were performed in accordance with Guide for the Care and Use of Laboratory Animals, and were approved by Animal Care and Ethical Committee of Hebei Medical University.

Microinjection of saporin conjugate into the NTS

Microinjections of the toxin substance P-saporin (SSP-SAP; Advanced Targeting System, San Diego, CA, USA) were made in adult male wild-type of Phox2b-EGFP transgenic mice (25–30 g). The mice, mounted on a stereotaxic instrument (Stoelting Co., Wood Dale, IL, USA), were anaesthetized with halothane (4% induction followed by 1 to 1.5% maintenance) delivered in 100% O₂ by a nasal mask. Depth of anaesthesia was assessed by an absence of the corneal and hindpaw withdrawal reflex. All surgical procedures were performed under strict aseptic conditions. The occipital craniotomy was carried out to expose dorsal surface of the medulla oblongata over the NTS. A glass micropipette (~25 µm) filled with the toxins containing SSP-SAP or Blank-SAP dissolved in PBS was injected into the dorsal and medial portions of the NTS at the level of calamus scriptorius (medial/lateral ± 0.3 mm, anterior/posterior 0.2 mm, dorsal/ventral –0.2 mm; medial/lateral ± 0.4 mm, anterior/posterior 0.3 mm, dorsal/ventral –0.3 mm) using a syringe pump (Harvard Apparatus, Holliston, MA, USA). Two protocols were applied for SSP-SAP injections. In immunostaining experiments, to determine how many Phox2b-containing cells were destroyed, a total volume of 100 nl of PBS containing 6 ng of SSP-SAP (3 ng in 50 nl; two injections) was injected into one side of the NTS and the contralateral NTS was used as a control (no injection). For *in vivo* experiments, to determine whether loss of Phox2b cells led to impaired HCVR, we injected bilaterally the total volume of 200 nl of PBS containing 6 ng (1.5 ng in 50 nl per injection; two injections per side) or 12 ng (3 ng in 50 nl per injection; two injections per side) of toxin into NTS. Therefore, the number of cells counted in mice injected bilaterally with 200 nl (12 ng) is approximately twice that of mice injected

unilaterally with 100 nl (6 ng). Blank-SAP (bilateral, 6 ng on each side) is non-targeted via non-specific peptide conjugated to saporin. This was used as a control for any non-specific effects of the toxin and provided a baseline for determining the effects of the SSP-SAP. The pipette was left *in situ* for 10–15 min to avoid efflux of the toxin. After injection, mice received postoperative boluses of atipamezole (α_2 -adrenergic antagonist, 2 mg kg⁻¹, s.c.), ampicillin (125 mg kg⁻¹, i.p.) and ketoprofen (4 mg kg⁻¹, s.c.). Ampicillin and ketoprofen were re-administered 24 hours postoperatively. Mice were then maintained for 2 weeks before breathing measurements. The toxin produced no observable behavioural effects or toxicity, regardless of dosage. No mice died from injection of the toxin. The doses of SSP-SAP were chosen in accordance with a previous study reporting on the effect of injection of SSP-SAP into the NTS on cardiovascular reflexes (Lin *et al.* 2012, 2013).

Breathing measurements

The SSP-SAP-injected and control mice were subjected to bilateral transections of the carotid sinus nerves before injections of neurotoxin as previously described (Kumar *et al.* 2015). Briefly, the mice were anaesthetized with halothane as described above. Body temperature of all mice was maintained at 37°C using a temperature-controlled heating pad. The carotid body was approached via a posterior midline neck incision and the carotid sinus nerve branches were sectioned. The wound was carefully sutured and cleaned with 10% of polyvidone iodine. Chemodenervated mice were used for WBP 5–7 days post recovery. To confirm whether carotid sinus nerves were sectioned successfully, the ventilatory response was evaluated by inhaling 10% O₂.

Breathing was studied in conscious, freely moving mice treated with SSP-SAP and Blank-SAP by WBP (EMKA Technologies, Paris, France) as described previously (Kumar *et al.* 2015). In brief, mice were placed in the WBP chamber at least 2 h (acclimation period) before the testing protocol. The typical protocol consisted of four sequential incremental CO₂ challenges (7 min exposures to 0%, 2%, 4%, 6% and 8% CO₂, balance O₂; each separated by 5 min of 100% O₂). The concentrations of CO₂ was measured and consecutively monitored with a capnograph (CWE Incorporated, Akron, OH, USA). A mass flow regulator provided quiet, constant and smooth flow through the animal chamber (0.5 l min⁻¹). Ventilatory flow signals were recorded, amplified, digitized and analysed using IOX 2.7 (EMKA Technologies) to determine ventilatory parameters over sequential 20 s epochs (~50 breaths), during periods of behavioural quiescence and regular breathing. Minute volume (MV; ml min⁻¹ g⁻¹) was calculated as the product of the respiratory frequency (breaths min⁻¹) and tidal volume

(TV; $\mu\text{l g}^{-1}$), normalized to mouse body weight (g). Note that the respiratory function test was carried out in chemodenervated mice unless indicated otherwise.

Electrophysiology

Protocols have been described in detail previously (Wang *et al.* 2013a, b). Briefly, transverse brainstem slices were made acutely from Phox2b-EGFP transgenic mice (P7-11) of either sex after decapitation under deep anaesthesia (5% pentobarbital sodium at 1.5 ml kg^{-1}). The brainstem was removed and coronal slices ($250 \mu\text{m}$, thickness) were cut with a vibrotome (VT1200S; Leica Biosystems, Wetzlar, Germany) in an ice-cold sucrose-containing solution (in mM: 260 sucrose, 3 KCl, 2 MgCl_2 , 2 CaCl_2 , 1.25 NaH_2PO_4 , 26 NaHCO_3 , 1 glucose and 1 kynurenic acid). Slices were then incubated for 30 min at 37°C and subsequently at room temperature in normal Ringer solution containing the ingredients (in mM): 130 NaCl, 3 KCl, 2 MgCl_2 , 2 CaCl_2 , 1.25 NaH_2PO_4 , 26 NaHCO_3 and 10 glucose. Slices were allowed for at least 1 hour of recovery before recording. All cutting and incubation solutions were bubbled with 95% O_2 and 5% CO_2 .

To obtain dissociated NTS neurons, thick slices ($350\text{--}400 \mu\text{m}$, thickness) were cut and maintained at room temperature for 15 min in PIPES buffer solution containing (in mM): 120 NaCl, 5 KCl, 1 MgCl_2 , 1 CaCl_2 , 25 glucose and 20 PIPES, bubbled with 100% O_2 , and then for 70–80 min at 33°C in PIPES containing trypsin (type XI; 0.5 mg ml^{-1} ; Sigma-Aldrich, Shanghai, China). After enzymatic digestion, slices were washed and maintained in PIPES buffer at room temperature for ~ 60 min. After transferring to Dulbecco's modified Eagle's medium (Thermo Fisher Scientific Inc., Beijing, China), the NTS region was identified with a dissecting microscope and cut carefully using a fine scalpel. In this line of transgenic mice, EGFP was expressed not only in the NTS but also the dorsal motor nucleus of vagus (DMNV) and area postrema (AP). To guarantee most patched cells from NTS, great care was taken to excise DMNV and AP from the NTS region. The tissue mainly containing the NTS was then triturated gently by a series of fire-polished Pasteur pipettes (inner diameter 600, 300 and $150 \mu\text{m}$). The suspension was allowed to settle for ~ 10 min in a recording chamber on a fixed-stage fluorescence microscope (Optical BX51WI; Olympus, Tokyo, Japan) equipped with infrared optics before electrophysiological recordings.

Cell-attached and whole-cell recordings were made in EGFP-expressing neurons at room temperature using pClamp, a Multiclamp 700B amplifier and a Digidata 1440A analog-to-digital converter (all from Molecular Devices, Sunnyvale, CA, USA) in a bath solution that was superfused continuously at a speed of 2 ml min^{-1} . The patch pipettes ($3\text{--}6 \text{ M}\Omega$) were filled with (in mM): 120 KCH_3SO_3 , 4 NaCl, 1 MgCl_2 , 0.5 CaCl_2 , 10 HEPES,

10 EGTA, 3 Mg-ATP and 0.3 GTP-Tris, pH adjusted to 7.2 with KOH. Bath solution consisted of HEPES-based solution (in mM: 140 NaCl, 3 KCl, 2 MgCl_2 , 2 CaCl_2 , 10 HEPES and 10 glucose, pH adjusted by adding HCl and NaOH) and bicarbonate-based buffer (normal Ringer solution) bubbled with 95% $\text{O}_2/5\%$ CO_2 (pH ~ 7.3) and 92% $\text{O}_2/8\%$ CO_2 (pH ~ 7.1). All recordings in brain slices were made in the presence of bicuculline (10 mM) and 6-cyano-7-nitroquinoxaline-2,3-dione (10 mM) in the bath solution to block fast excitatory and inhibitory synaptic transmissions. Cell-attached recordings were made at a holding potential of -60 mV , and recordings of membrane potential and action potential discharge were obtained by whole-cell current clamp. Firing rate histograms were generated by integrating action potential discharge in 10 s bins using Spike2 software (Cambridge Electronic Design, Cambridge, UK). Under whole-cell voltage clamp, cells were recorded at a holding potential of -60 mV . The current–voltage (I – V) relationships from under control conditions and bath acidification were determined using voltage steps between -60 to -120 mV (10 mV increment). Chemicals were purchased from either Sigma-Aldrich or Tocris Bioscience (Shanghai, China).

Immunofluorescence staining

Mice were anaesthetized with an overdose of urethane (1.8 g kg^{-1} , i.p.) and then perfused through the ascending aorta with 200 ml of PBS (pH 7.4), followed by 4% phosphate-buffered (0.1 M, pH 7.4) paraformaldehyde. The mouse was decapitated, and the brainstem was dissected and stored in the perfusion fixative for 24–48 h at 4°C . Following dehydration by ethanol and xylene, the tissue was embedded in paraffin. A microtome (Leica Biosystems) was used to cut the embedded tissue into sections ($5 \mu\text{m}$ thickness), followed by mounting sections onto gelatin coated slides for drying overnight. After that, the tissue sections were deparaffinized and rehydrated by sequentially immersing the slides into xylene, ethanol and distilled water, further followed by antigen retrieval using microwave. Tissue sections were then treated with 0.3% Triton X-100 in PBS before blocking any non-specific binding by incubating the tissue sections with 2% BSA for 30 min at room temperature. For immunofluorescence staining, the sections were incubated with primary antibodies in 2% BSA at 4°C overnight, followed by thorough rinsing with PBS. The affinity-purified fluorescence dye conjugated secondary antibodies were then incubated with sections at room temperature for 1–1.5 hours. Finally sections were washed, air-dried, and mounted on slides with Vectashield Antifade Mounting Medium (Vector Laboratories, Burlingame, CA, USA) for visualization. The Phox2b was detected with a mouse monoclonal antibody (dilution 1:1000,

sc-376993; Santa Cruz Biotechnology, Inc., Santa Cruz, CA, USA), NTS neurons with the neuronal marker neuronal nuclear antigen (NeuN) (dilution 1:500, ab177487; Abcam, Shanghai, China), cFos with a rabbit antibody (dilution 1:200, #2250; Cell Signaling Technology, Danvers, MA, USA) and EGFP with a chicken antibody (dilution 1:500, ab13970; Abcam). These primary antibodies were detected by incubation with matched secondary antibodies tagged with fluorescence reporters to reveal Phox2b (dilution 1:200, goat anti-mouse Cy3 or donkey anti-mouse FITC; Jackson Laboratories Inc., West Grove, PA, USA), NeuN (dilution 1:400, donkey anti-rabbit Cy3; Jackson Laboratories Inc.), EGFP (dilution 1:200, goat anti-chicken Alexa Fluor488; Abcam) and cFos (dilution 1:200, donkey anti-rabbit FITC; Jackson Laboratories Inc.). The substance P receptor (neurokinin-1 receptor, NK1R) was detected with a guinea pig antibody (dilution 1:2000, #AB15810; EMD Millipore Corporation, Darmstadt, Germany) and revealed with goat anti-guinea pig Cy3 (dilution 1:200; Jackson Laboratories Inc.). Stained sections were imaged using a DM6000B fluorescence microscope (Leica Microsystems). Images were acquired and processed with the Leica Application Suit, version 4.6. The uninjected side of each section served as intratissue and as intra-animal control for the injected side.

For cFos-based histological analysis of CO₂-activated neurons, mice were first subjected to unilateral micro-injections of SSP-SAP (6 ng). After 2 weeks, mice were placed in the plethysmography chamber and then exposed to the 8% CO₂ stimulus (hyperoxic hypercapnia) for 60 min, followed by 60 min of hyperoxia. Immediately after the hypercapnic exposure, the mice were anaesthetized and perfused transcardially with fixative for subsequent histological processing as described above.

To visualize whether EGFP-labelled neurons were physically isolated from astrocytes, after dissociation of NTS neurons as depicted above, the suspension containing neurons and glia cells was allowed to settle down for 10–15 min on a coverslip placed in a dish. After gentle washes with PBS, the coverslips were incubated with 4% paraformaldehyde for 10 min and subsequently with 0.5% Triton X-100 in PBS for 5 min. Incubation was continued with 2% BSA for 1 h at room temperature. The subsequent steps of antibody incubation were similar to the protocol described above. Astrocytes were detected with a rabbit anti-GFAP antibody (dilution 1:5000, ab7260; Abcam, Shanghai, China) and EGFP with a chicken antibody (dilution 1:500) as used above.

Statistical analysis

Statistical analysis was done with Prism, version 6 (GraphPad Software, Inc., La Jolla, CA, USA). Data are reported as the mean \pm SEM. To compare the difference

in the number of cells between control and injection sides, a two-tailed paired *t* test or one-way ANOVA was used. Breathing measurements were analysed by two-way ANOVA with *post hoc* multiple comparison tests. For electrophysiological experiments, a two-tailed paired *t* test was used to determine significance. $P < 0.05$ was considered statistically significant.

Results

SSP-SAP ablates Phox2b-expressing NTS neurons

SSP-SAP is a neurotoxin that selectively ablates NK1R-containing neurons via inactivation of the ribosome. To assess whether Phox2b and NK1R were co-expressed in NTS neurons, double-immunofluorescence staining was carried out in eight consecutive coronary sections per mice ($n = 6$). As shown in Fig. 1A, NK1Rs, like Phox2b, were present in the NTS and DMNV neurons. According to cell counts (Fig. 1B), almost 90% of NK1R⁺ NTS neurons were immunoreactive for Phox2b, in contrast, ~80% of Phox2b⁺ neurons for NK1R, in favour of high co-expression of two molecules. Therefore, this pattern of high co-expression provided a strong reliability for effective lesions of Phox2b⁺ neurons with SSP-SAP. To determine what proportion of NTS neurons were Phox2b⁺, double-labelling of Phox2b and NeuN was performed in eight consecutive coronary sections per mice ($n = 4$). As shown in Fig. 1C and D, almost all Phox2b⁺ neurons were immunoreactive for NeuN and Phox2b-containing neurons accounted for ~69% of NeuN-labelled cells in the NTS based on cell counts.

To determine the most effective dose required for functional deficiency, SSP-SAP (3 and 6 ng) was unilaterally microinjected into the NTS. Phox2b immunoreactivity was examined to assess the effect of SSP-SAP on Phox2b⁺ NTS neurons and neighbouring DMNV neurons. Phox2b⁺ neurons were counted in eight consecutive coronal sections of each mouse ($n = 3$). The rostrocaudal position of each coronal section was determined (bregma: -7.08 to -7.92 mm, approximately corresponding to caudal and intermediate NTS) in light of the atlas of *The Mouse Brain in Stereotaxic Coordinates* (Paxinos & Franklin, 2003). Figure 2A illustrates a typical outcome of the unilateral microinjection of SSP-SAP (6 ng), which reduced the number of Phox2b⁺ neurons on injection side compared to the control side. Cell counts were obtained on control and injection sides, respectively, aiming to assess how many Phox2b⁺ neurons were eliminated. Group data (Fig. 2B and C) demonstrated that 87% of Phox2b⁺ neurons were retained in 24 sections from three mice (eight sections per mouse) after administration of 3 ng of SSP-SAP (1118 ± 59 vs. 973 ± 51 , control vs. SSP-SAP, $P < 0.01$). The 6 ng dose of toxin further reduced Phox2b⁺ neurons to 82% of control

(1155 ± 20 vs. 952 ± 16 , control vs. SSP-SAP, $P < 0.01$). However, unilateral injection of Blank-SAP (6 ng) into the NTS had no remarkable effect on the number of Phox2b⁺ neurons (data not shown). Care was taken to avoid the destruction of DMNV neurons by placing microinjections in the NTS only. As a result, the 6 ng dose of SSP-SAP was without considerable destruction of DMNV neurons (Fig. 2D and E).

NTS lesions attenuate the ventilatory response to CO₂

To examine whether Phox2b-expressing NTS neurons contributed to the regulation of breathing, lung function was measured using WBP in conscious chemodenervated mice treated with SSP-SAP when the mice were quietly resting. The ventilation was assessed by comparing the difference in TV, breathing frequency and MV between SSP-SAP-injected mice and counterparts, in response to hyperoxic hypercapnia by inhaling different concentrations of CO₂ (2% CO₂, low level of hypercapnia; 4–6% CO₂, moderate level of hypercapnia; 8% CO₂, high level of hypercapnia). As shown in Fig. 3,

when exposed to normocapnia (100% O₂), no statistical difference was found in breathing parameters in mice treated with injection of either 6 ng ($n = 13$) or 12 ng ($n = 12$) of SSP-SAP compared to control mice ($n = 13$). When challenged by hypercapnia, both control and SSP-SAP-injected mice exhibited an increased TV, breathing frequency and therefore an increased MV. However, the hypercapnia-elicited increase in ventilation was reduced to a different degree in SSP-SAP-injected mice. Compared to control mice, the injection of a 6 ng dose of SSP-SAP was ineffective on changes in breathing parameters when challenged by 2%, 4% and 6% CO₂ ($P > 0.05$ for all), with the exception that the ventilation was reduced during exposure to 8% CO₂, as expressed by TV (18.6 ± 1.1 vs. 16.3 ± 0.4 $\mu\text{l g}^{-1}$, control vs. 6 ng of SSP-SAP, $P < 0.05$) (Fig. 3A) and MV (4.20 ± 0.15 vs. 3.67 ± 0.13 $\text{ml min}^{-1} \text{g}^{-1}$, control vs. 6 ng of SSP-SAP, $P < 0.01$) (Fig. 3C). Apparently, MV and TV were both reduced by 13% during exposure to 8% CO₂ in inspired air when $\sim 13\%$ of the Phox2b-expressing neurons were eliminated. Furthermore, in the mice treated with 12 ng of SSP-SAP, the increase in TV was lower

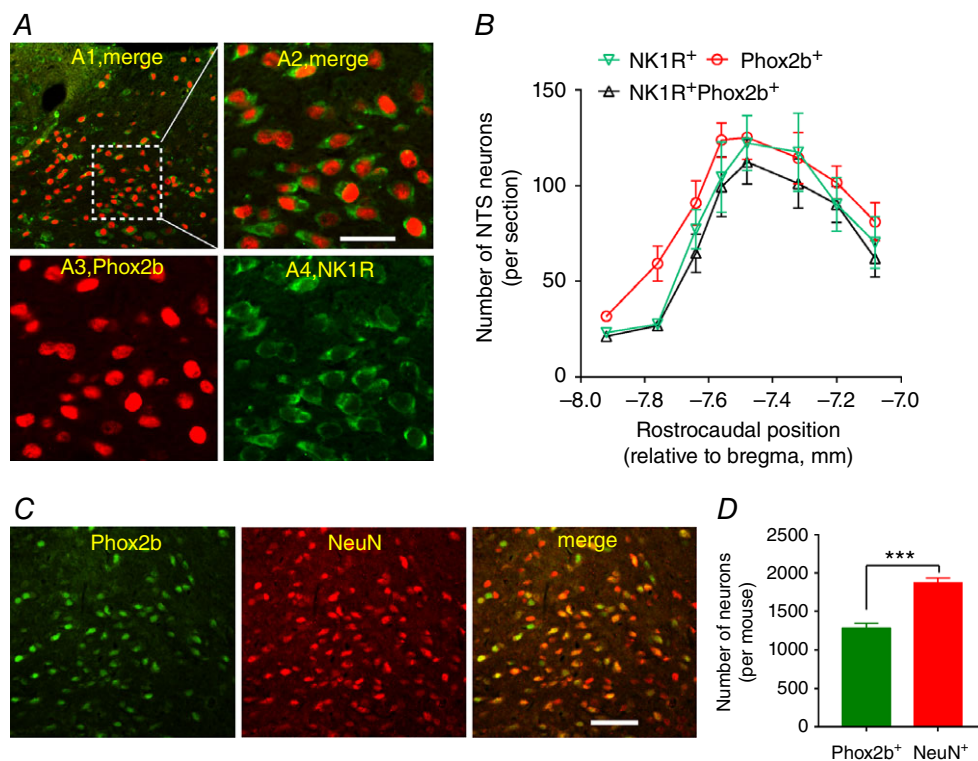


Figure 1. Characteristics of Phox2b and NK1R expression in NTS neurons

A, photomicrographs showing immunoreactivity for Phox2b and NK1R. A1, co-expression of Phox2b and NK1R. The inset is enlarged in a merged image (A2). Nuclear Phox2b immunoreactivity (red, A3) was co-localized (A2) in most of the neurons with membrane-bound NK1R immunoreactivity (green, A4). B, rostrocaudal distribution of NK1R⁺, Phox2b⁺ and NK1R⁺Phox2b⁺ neurons. Unilateral cell counts were obtained from eight consecutive coronal sections from each mouse ($n = 6$). C, immunofluorescence labelling indicating immunoreactivity for Phox2b (green) and NeuN (red) in the NTS. Both represent nuclear localization. D, the number of Phox2b⁺ cells is less than that labelled by NeuN. Cells were counted unilaterally using the same protocol as B. Scale bar = 50 μm . *** $P < 0.001$ by unpaired *t* test. [Colour figure can be viewed at wileyonlinelibrary.com]

even during exposure to 4% CO₂ ($9.0 \pm 0.5 \mu\text{l g}^{-1}$), as well as 6% ($11.9 \pm 0.5 \mu\text{l g}^{-1}$) and 8% CO₂ ($13.8 \pm 0.6 \mu\text{l g}^{-1}$), whereas in control mice, the values of TV were $11.6 \pm 1.0 \mu\text{l g}^{-1}$ for 4% CO₂ ($P < 0.05$), $15.6 \pm 1.2 \mu\text{l g}^{-1}$ for 6% CO₂ ($P < 0.001$) and $18.6 \pm 1.1 \mu\text{l g}^{-1}$ for 8% CO₂ ($P < 0.001$) (Fig. 3A), respectively. Thus, the increase in MV was also lower in mice treated with 12 ng of SSP-SAP than those in the control group during exposure to 4% (1.98 ± 0.13 vs. $1.43 \pm 0.05 \text{ ml min}^{-1} \text{ g}^{-1}$, control vs. 12 ng of SSP-SAP, $P < 0.001$), 6% (3.38 ± 0.13 vs. $2.54 \pm 0.14 \text{ ml min}^{-1} \text{ g}^{-1}$, control vs. 12 ng of SSP-SAP, $P < 0.001$) and 8% CO₂ (4.20 ± 0.15 vs. $3.23 \pm 0.14 \text{ ml min}^{-1} \text{ g}^{-1}$, control vs. 12 ng of SSP-SAP, $P < 0.001$) (Fig. 3C). Consequently, loss of ~18% of Phox2b-containing neurons was associated with remarkable decreases in MV by $\geq 18\%$ and in TV by $\geq 22\%$ when challenged by $\geq 4\%$ CO₂. In both cases,

breathing frequency was unchanged between control and SSP-SAP-injected mice (Fig. 3B). To understand the relationship between the number of Phox2b-expressing neurons and HCVR, we made a linear regression analysis. As shown in Fig. 3D, the number of Phox2b-containing cells has a marked impact on MV at high level of hypercapnia ($P < 0.001$).

To test whether activation of peripheral chemoreceptors affected HCVR through synaptic connections following lesions of Phox2b⁺ neurons, breathing parameters were measured in a number of carotid body innervated mice. However, no noticeable difference in MV was found during exposure to up to 8% CO₂ between carotid body innervated and denervated mice (data not shown), as well as between two groups after injections of SSP-SAP (Fig. 3E). The successful carotid body denervation was confirmed by a hypoxic ventilatory response (Fig. 3F).

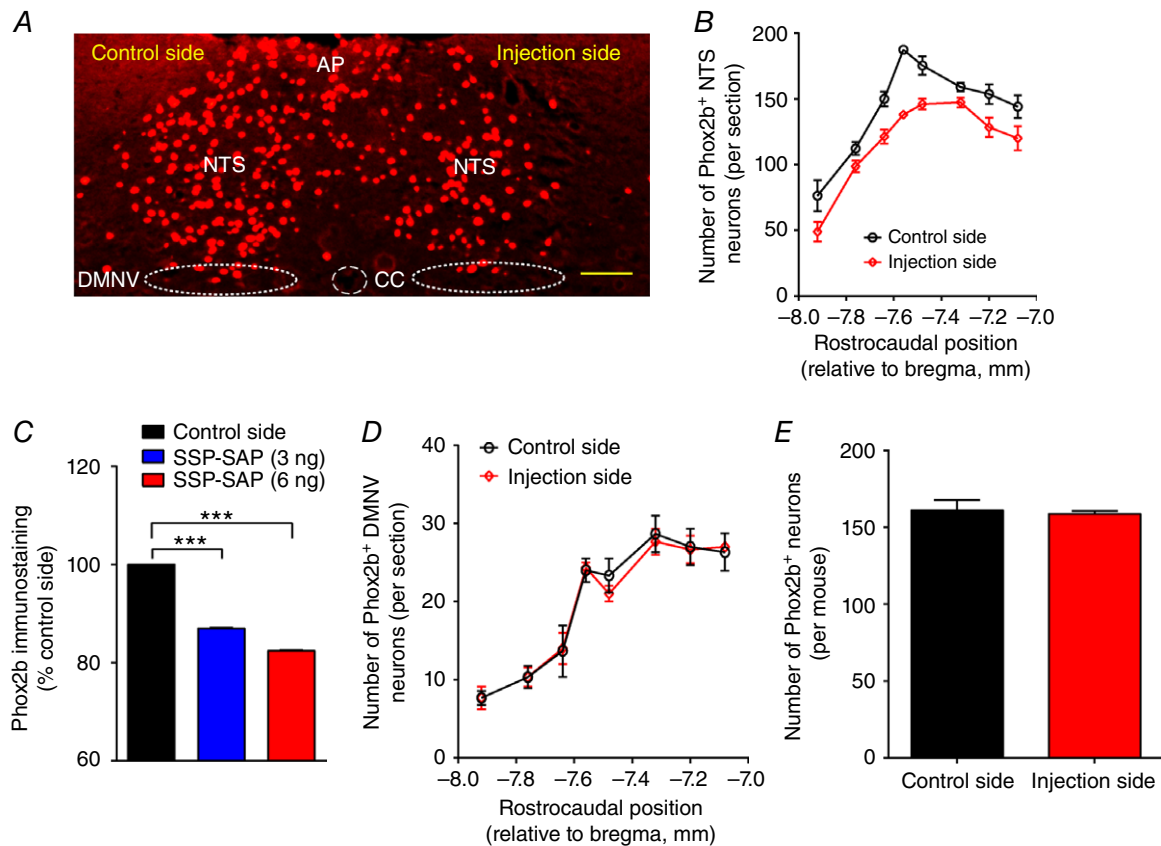


Figure 2. SSP-SAP destroys Phox2b⁺ neurons effectively

A, representative photomicrograph of immunofluorescence staining showing the effect of unilateral injection of 6 ng of SSP-SAP on Phox2b⁺ neurons. Phox2b⁺ nuclei are denoted in red (Cy3 fluorescence). Scale bar = 100 μm . B, rostrocaudal distribution of the Phox2b⁺ neurons on control and injection sides. Cell counts were obtained from eight consecutive coronal sections from each mouse ($n = 3$) subjected to injection of 6 ng of SSP-SAP. Section alignment was done using as reference the coronal sections located between bregma -7.08 to -7.92 mm. C, effect of injection of 3 and 6 ng of SSP-SAP on Phox2b⁺ neurons. Each column represents the total number of Phox2b⁺ neurons in eight consecutive coronal sections of each mouse ($n = 3$). *** $P < 0.001$ by one-way ANOVA with Tukey's *post hoc* test. D, rostrocaudal distribution of the Phox2b⁺ DMNV neurons on control and injection sides in mice ($n = 3$) treated with 6 ng of SSP-SAP. E, injection of 6 ng of SSP-SAP is without significant effects on Phox2b⁺ neurons in the DMNV. CC, central canal. [Colour figure can be viewed at wileyonlinelibrary.com]

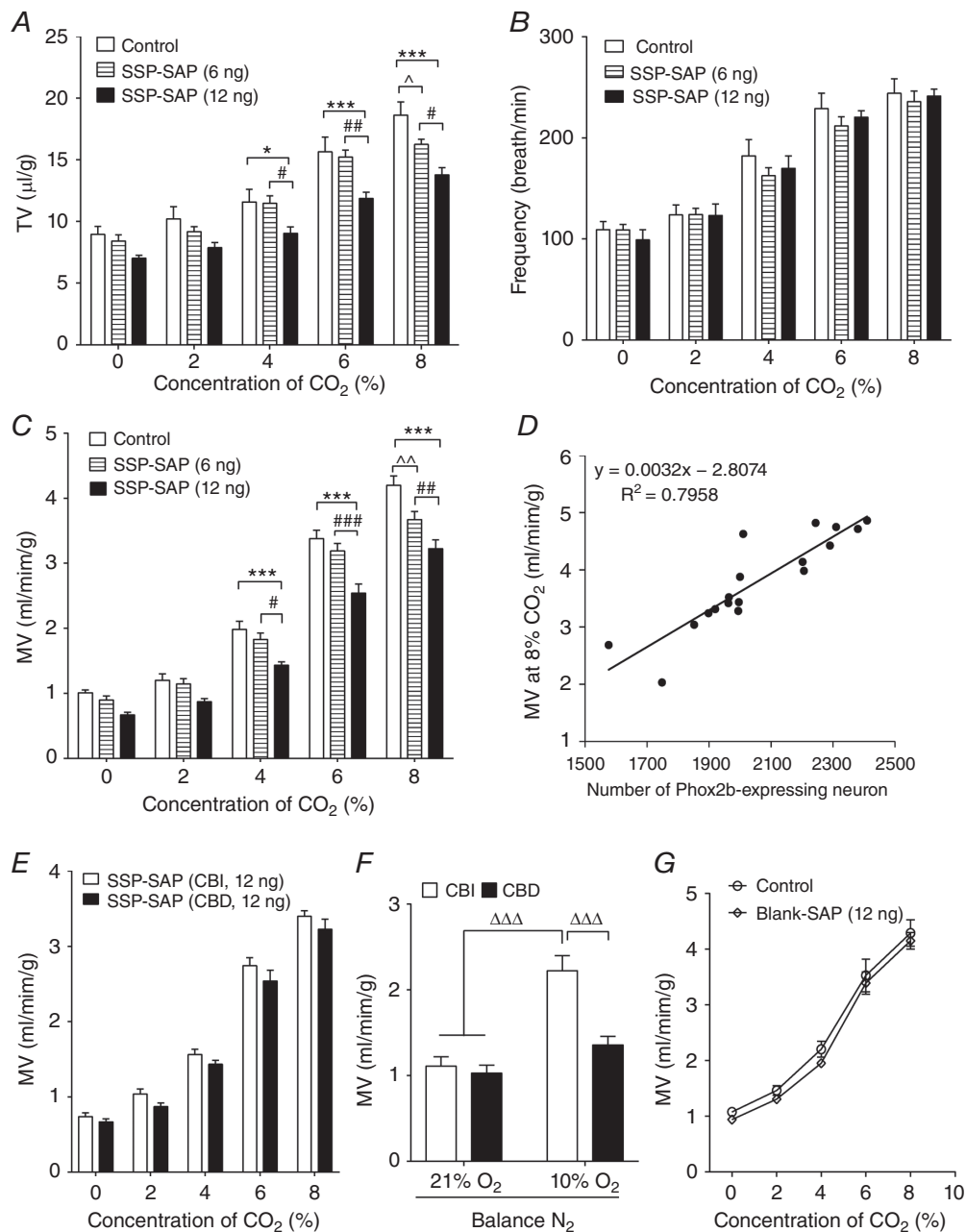


Figure 3. Loss of Phox2b-expressing neurons attenuates HCVR

A–C, pooled data showing the effects during wakefulness of bilateral injections of SSP-SAP on TV (A), respiratory frequency (B) and MV (C) at different CO₂ concentrations in the inspired air (balance O₂). * $P < 0.05$, *** $P < 0.001$, vs. control; # $P < 0.05$, ## $P < 0.01$, ### $P < 0.001$, vs. 6 ng SSP-SAP; $\hat{P} < 0.05$, $\tilde{P} < 0.01$, vs. control, two-way ANOVA with Tukey's *post hoc* test ($n = 13$ for control, $n = 13$ for 6 ng, $n = 12$ for 12 ng). D, linear regression analysis of hypercapnic ventilation and the number of Phox2b-containing cells. The number of Phox2b cells was counted from eight consecutive sections of each control and SSP-SAP (12 ng)-injected mice ($n = 9$ for each group). MV was measured during exposure to 8% CO₂ in corresponding mice. The scatter chart was plotted using MV against the number of Phox2b cells and a trending line was added. $r^2 = 0.7958$, $P < 0.001$ by ANOVA. E, CBI and CBD mice exhibited similar increases in MV during exposure to CO₂ after injection of 12 ng of SSP-SAP ($n = 12$ for both). $P > 0.05$ for all by two-way ANOVA with Bonferroni's test. CBI, carotid body innervated; CBD, carotid body denervated. F, CBD mice displayed a blunted ventilation during exposure to 10% O₂ compared to CBI ($n = 8$ for CBI, $n = 7$ for CBD). $\Delta\Delta\Delta P < 0.001$ by two-way ANOVA with Tukey's *post hoc* test. G, bilateral injections of 12 ng of Blank-SAP are without effects on MV.

To determine the selectivity of SSP-SAP and to rule out any non-specific effects of this toxin, injection of Blank-SAP (12 ng) produced no significant effects on MV (Fig. 3G). Collectively, the WBP experiments suggest that the attenuated HCVR is more plausibly the result of a loss of Phox2b-expressing neurons in the NTS.

SSP-SAP destroys CO₂-activated NTS neurons

To determine whether the respiratory deficits caused by injection of SSP-SAP were mainly caused by loss of CO₂-activated NTS neurons, the immunoreactivity to cFos was examined in mice following injection of SSP-SAP. Immunofluorescence staining was performed in 24 sections from three mice (Bregma: -7.08 to -7.92 mm, eight sections per mouse) subjected to unilateral injection

of 6 ng of SSP-SAP. As shown in Fig. 4A, the CO₂-activated NTS neurons were identified by immunoreactivity to cFos (cFos⁺) and were denoted in green. Obviously, the number of Phox2b⁺cFos⁺ neurons was considerably decreased on the injection side compared to the contralateral side. The total number of cFos⁺ cells on the injection side was far less than that on the control side (141 ± 8 vs. 91 ± 3 , control side vs. injection side, $n = 3$ mice, $P < 0.01$). Furthermore, the total number of Phox2b⁺cFos⁺ neurons on the injection side was also reduced compared to the control side (105 ± 8 vs. 71 ± 8 , control side vs. injection side, $n = 3$ mice, $P = 0.044$) (Fig. 4B and C). In addition, the Phox2b⁺cFos⁺ neurons accounted for $\sim 74\%$ of cFos⁺ and for $\sim 10\%$ of Phox2b⁺ neurons on the control side, respectively, suggesting that a large fraction of cFos⁺ neurons were immunoreactive to Phox2b.

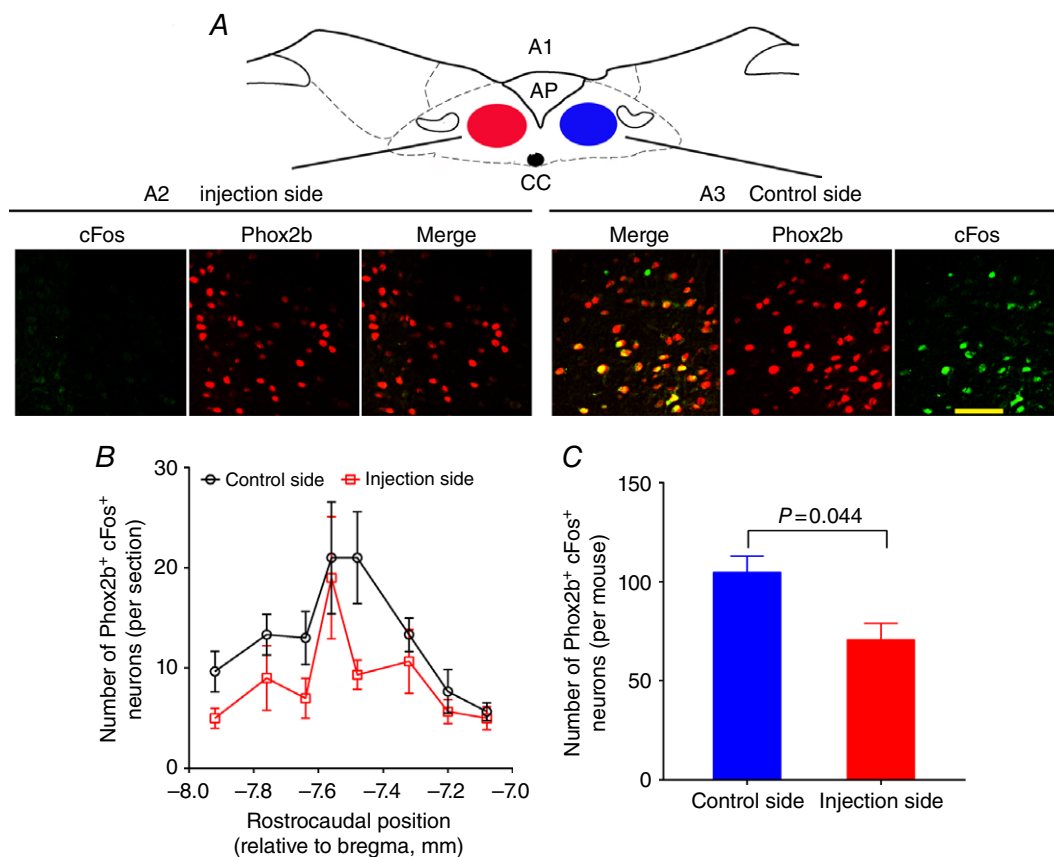


Figure 4. Effect of injection of SSP-SAP on CO₂-activated NTS neurons

A, typical immunofluorescence photomicrographs showing cFos⁺(green), Phox2b⁺ (red) and Phox2b⁺cFos⁺ (merge) neurons in a coronal section from a mice treated with unilateral injection of 6 ng of SSP-SAP. The mouse was exposed to 8% CO₂ and CO₂-activated neurons were detected with cFos⁺. A1, coronary schematic sketch of a brainstem section (bregma -7.64 mm). Images (A2 and A3) are enlarged from the NTS regions indicated by red and blue ovals (A1). The number of Phox2b⁺cFos⁺ neurons is greater on the control side (A3) compared to the injection side (A2). Scale bar = 50 μ m. B, rostrocaudal distribution of Phox2b⁺cFos⁺ neurons counted from eight consecutive coronal sections per mouse ($n = 3$). C, pooled data showing the effect of unilateral injection of 6 ng of SSP-SAP on Phox2b⁺cFos⁺ neurons. Each column represents the total number of Phox2b⁺ neurons in eight consecutive coronal sections of each mouse. $P = 0.044$ by a two-tailed paired t test. [Colour figure can be viewed at wileyonlinelibrary.com]

Intrinsic chemosensitivity of Phox2b-expressing NTS neurons *in vitro*

We assumed that the blunted HCVR caused by SSP-SAP was the result of a loss of chemosensitive Phox2b-expressing neurons. Therefore, an experiment was carried out aiming to characterize chemosensitivity of this group of neurons in Phox2b-EGFP transgenic mice. In the dorsal medulla of this transgenic mouse line, EGFP was mainly expressed in the NTS, DMNV and AP. Using double-immunohistochemical staining, we found that 100% of EGFP-expressing neurons were immunoreactive to Phox2b ($n = 515$ from three mice) (Fig. 5A).

Effects of bath acidification on firing activity of Phox2b-expressing NTS neurons. To examine whether Phox2b-expressing NTS neurons were sensitive to CO_2/H^+ in the presence of blockade of fast synaptic transmissions, cell-attached recordings were made from directly visualized neurons in acute brainstem slices from Phox2b-EGFP mice. Only EGFP-labelled neurons with spontaneous discharge were chosen for testing chemosensitivity. Chemosensitive neurons were defined as those exhibiting $> 30\%$ increases in firing rate at bath pH 7.0 (or 8% CO_2) relative to that at pH 7.4 (or 5% CO_2). Of 79 Phox2b-expressing NTS neurons, 43% ($n = 34$) displayed chemosensitive responses, whereas the firing rate was unchanged ($n = 37$) or reduced ($n = 8$) during bath acidification in the remaining 57% cells ($n = 45$). The pH-sensitive neurons were mostly located in the medial, intermedial and dorsal parts of the NTS (Fig. 5C).

Under cell-attached conditions, we defined two different responsive modes in neurons superfused by the HEPES-based buffer. In one set of neurons, the firing rate increased from 1.5 ± 0.3 at bath pH 7.4 to 2.7 ± 0.4 Hz at bath pH 7.0 ($n = 14$, $P < 0.001$) (Fig. 5D and E) and remained elevated during the whole period of acidification (Fig. 5D). In the other group, neurons fired from 1.0 ± 0.3 at bath pH 7.4 to 1.8 ± 0.4 Hz at bath pH 7.0 ($n = 10$, $P < 0.001$) (Fig. 5F and G). However, the enhanced activity of these cells was transient, followed by a swift return to the basal level (Fig. 5F). The average duration of the peak firing rate was 58 ± 8 s ($n = 10$).

Next, we examined CO_2 action on firing activity in a small number of neurons. Likewise, the firing rate was raised from 1.2 ± 0.4 at 5% CO_2 bubbled bicarbonate buffer solution (\sim pH 7.3) to 2.3 ± 0.6 Hz ($n = 6$, $P < 0.05$) at 8% CO_2 (\sim pH 7.1) in neurons exhibiting a 'sustained response' (Fig. 6A and B), as well as from 1.2 ± 0.3 at 5% CO_2 to 2.0 ± 0.6 Hz ($n = 4$, $P = 0.046$) at 8% CO_2 in those with a 'transient response' (Fig. 6C).

Dissociated NTS neurons retained pH sensitivity. As studied above, although the pH sensitivity of Phox2b-expressing NTS neurons was confirmed in

the presence of pharmacological blockade of synaptic transmissions in brain slices, it could not rule out the contribution of paracrine signalling derived from glia and vascular endothelium. To examine whether such pH sensitivity was an inherent feature, cell-attached recordings were made in acutely dissociated EGFP-expressing neurons. The patched cell was chosen in terms of morphological contour, such as cells with clean surface (no black dots), oval shape with three dimensions, processes, etc. Importantly, no detectable tissues (e.g. glia) were attached to the patched cell to enable an entirely physical isolation (Fig. 7B). In addition, the NTS cell was identified and patched in terms of its medial size discriminated from the big size of DMNV and from small size of AP cells. Having met the above criterion, bath acidification produced a remarkably increase in firing rate in 15 of 37 ($\sim 41\%$) cells, with decreased ($n = 18$) and unchanged ($n = 4$) firing in the rest of the cells. Consistent with pH-sensitive responses in slices, the firing rate increased from 2.4 ± 0.4 at pH 7.4 to 4.6 ± 0.8 Hz at pH 7.0 in cells with a 'sustained pattern' ($P < 0.001$, $n = 11$) (Fig. 7C and D), as well as from 3.0 ± 0.5 at pH 7.4 to 5.7 ± 1.1 Hz at pH 7.0 in those with a 'transient pattern' ($P < 0.05$, $n = 4$) (Fig. 7E). Taken together, the pH sensitivity was retained in dissociated EGFP-containing neurons.

Effect of bath pH alterations on membrane potential and firing activity. The two types of responses were probably mediated via different ion channels. For example, Huda *et al.* (2012) found that ASICs were responsible for chemosensitivity of NTS neurons exhibiting a 'transient response', although the ionic mechanism responsible for the 'sustained response' remains unanswered. To address this issue, we further tested pH sensitivity of NTS neurons with a 'sustained response' using whole-cell current clamp recording from EGFP-labelled neurons in brain slices. Bath acidification from pH 7.4 to pH 7.0 produced an average membrane depolarization with increased spontaneous discharge. As shown in Fig. 8A, a representative cell displayed membrane depolarization from -56 mV to -52 mV when challenged by bath acidification from pH 7.4 to pH 7.0, accompanied by an increase in firing rate. After returning to the initial bath pH 7.4, membrane potential and firing rate recovered to the baseline level, in favour of a reversible effect. Group data demonstrated an average amplitude of depolarization of 5 ± 1 mV and an average firing rate from 0.9 ± 0.2 at pH 7.4 to 2.0 ± 0.2 Hz at pH 7.0 ($n = 12$, $P < 0.001$) (Fig. 8B).

Characterization of pH-sensitive currents. To further characterize pH-sensitive currents, after cell-attached recordings demonstrating pH-sensitive responses in slices,

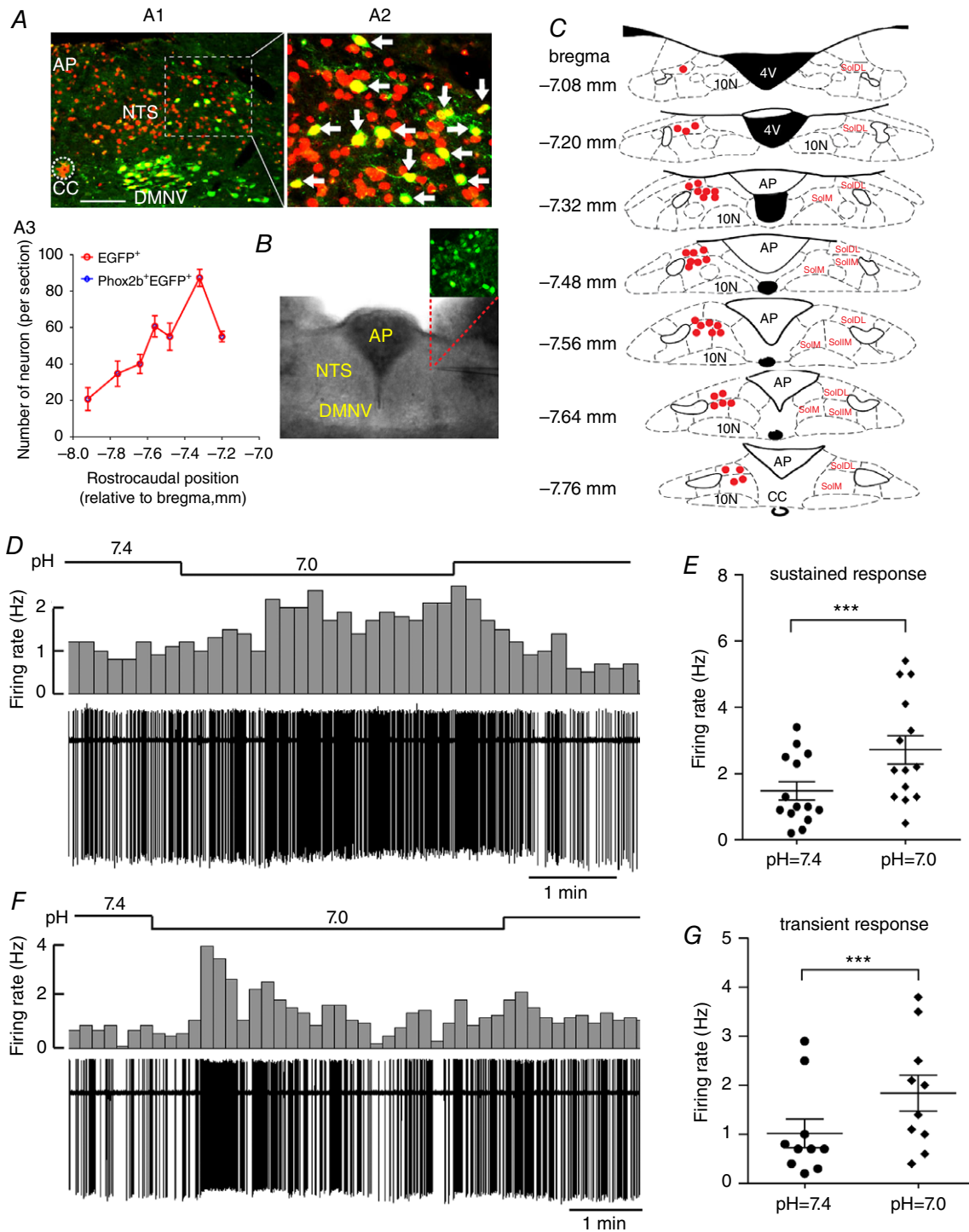


Figure 5. A subgroup of Phox2b-expressing neurons are sensitive to H⁺

A, each EGFP-expressing neuron is immunoreactive to Phox2b. A1, immunofluorescence photomicrograph showing the distribution of EGFP⁺ (green), Phox2b⁺ (red) and Phox2b⁺EGFP⁺ neurons (yellow, merged) in the NTS, DMNV and AP in a coronal section from a Phox2b-EGFP transgenic mouse. The inset is enlarged in (A2). Scale bar = 100 μm. A2, as indicated by white arrows, all of the EGFP⁺ neurons are immunoreactive to Phox2b. A3, rostrocaudal distribution of EGFP⁺ and Phox2b⁺EGFP⁺ neurons from three mice. B, image (bottom) of an acute brainstem slice containing NTS, with magnified fluorescence image (top) of EGFP-expressing neurons. C, distribution of pH-sensitive neurons in the NTS. After patch clamp recording, the location of each pH-sensitive EGFP-expressing neuron was pinpointed in the schematic sketch of the NTS based on the atlas of the *Mouse*

Brain in Stereotaxic Coordinates (Paxinos & Franklin, 2003). Red dots indicate the location of pH-sensitive cells. *D* and *F*, typical traces showing sustained (*D*) and transient (*F*) increases in firing rate during bath acidification in Phox2b-expressing neurons from Phox2b-EGFP mice. Firing rate histograms (top traces, 10 s bins) derived from cell-attached voltage clamp recordings (bottom traces). *E* and *G*, group data demonstrating sustained (*E*) ($n = 14$) and transient (*G*) ($n = 10$) increases in average firing rate during bath acidification in Phox2b-expressing neurons. *** $P < 0.001$ by a two-tailed paired t test. SolDL, dorsolateral part of the NTS; SolIM, intermediate part of NTS; SolM, medial part of the NTS. [Colour figure can be viewed at wileyonlinelibrary.com]

we then obtained whole-cell access and made voltage clamp recordings in these EGFP-labelled neurons. A wide range of pH values (6.8, 7.4 and 7.8) was applied to predict which ion channels contributed to the pH-sensitive currents. As shown in Fig. 9A, bath acidification to pH 6.8 elicited an inward shift at holding currents of -60 mV, whereas bath alkalization to pH 7.8 produced an outward shift. We plotted $I-V$ curve by digital subtraction of the current at pH 7.8 from that at pH 6.8. As shown in Fig. 9B, the average pH-sensitive current was weakly rectifying, with a reversal potential of ~ -85 mV, close to the predicted value of equilibrium potential of K^+ (-95 mV). It thus appears that these neurons possess a pH-sensitive background K^+ current.

Discussion

In the present study, we demonstrate that SSP-SAP destroys Phox2b⁺ neurons, particularly CO₂-activated Phox2b⁺ neurons in the NTS. Furthermore, lesions of Phox2b-expressing neurons are closely correlated with impaired HCVR in chemodenervated mice. These results extend previous evidence indicating that the NTS contributes to central respiratory chemoreflexes. We also demonstrate that a subgroup of Phox2b-expressing NTS neurons exhibits characteristic sensitivity to CO₂/H⁺,

which implicates that the Phox2b-expressing NTS neurons are candidate central respiratory chemoreceptors. These findings obtained *in vivo* and *in vitro* suggest that Phox2b-expressing NTS neurons are crucial for HCVR.

The respiratory deficits are attributable to the loss of Phox2b-expressing neurons

Because the development of the entire NTS is Phox2b-dependent (Dauger *et al.* 2003), it is possible that 100% of NTS neurons are Phox2b-contained. Previous evidence has demonstrated that Phox2b is almost exclusively associated with glutamatergic and not GABAergic neurons in the adult NTS (Kang *et al.* 2007), implying that a subset of NTS neurons do not contain Phox2b. Consistent with this finding, the present study indicates that Phox2b is present in $\sim 69\%$ of NTS neurons. It might be that Phox2b-expressing and non-Phox2b-expressing neurons contribute to the differential regulation of breathing in the NTS.

SSP-SAP has been employed to destroy reliably NK1R-expressing cells previously (Wiley & Kline, 2000), in particular in the NTS (Nayate *et al.* 2009; Lin *et al.* 2012) and RTN (Nattie & Li, 2002b; Takakura *et al.* 2008). In the present study, because of the feature of high co-expression of Phox2b and NK1R, the loss of Phox2b-containing NTS neurons is most probably attributed to injection of

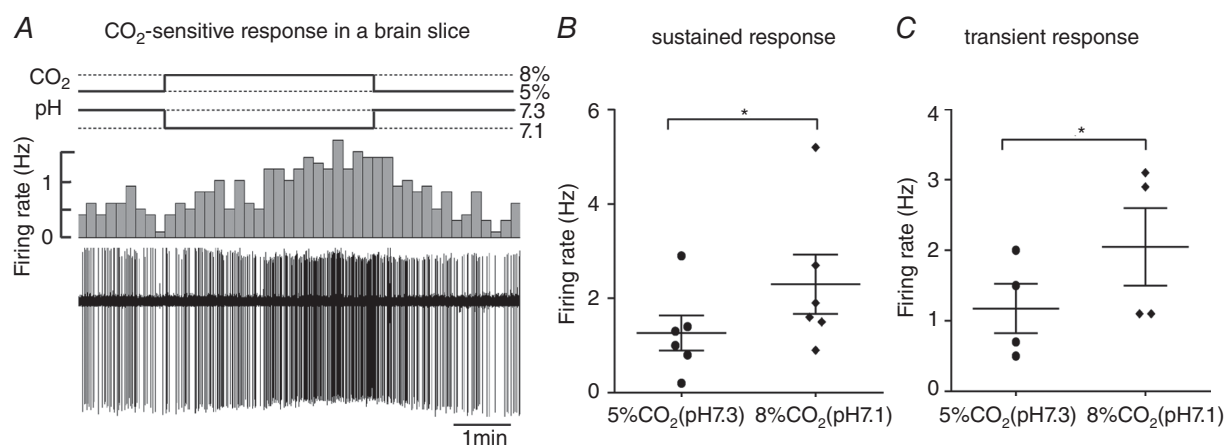


Figure 6. Effect of CO₂ on firing activity of Phox2b-expressing neurons

A, representative cell-attached recording of firing rate in response to changes in different concentrations of CO₂ from a Phox2b-expressing neurons in slices. Traces and histograms show a sustained increase in firing rate during 8% CO₂ bubbled bath solution (\sim pH 7.1). *B* and *C*, average firing rate during changes in pH produced by altering CO₂ concentrations in neurons with sustained (*B*) ($n = 6$) and transient (*C*) ($n = 4$) responses. * $P < 0.05$ by a two-tailed paired t test.

neurons is far greater than that in the RTN. Second, the blunted HCVR is accompanied by a diminished number of CO₂-activated Phox2b-expressing neurons. Taking into account the large number of Phox2b-expressing neurons, it is not surprising that not all of Phox2b⁺ neurons were CO₂-responsive in light of cFos immunoreactivity. Nevertheless, a large number of CO₂-activated neurons was immunoreactive for Phox2b. It is estimated that the loss of ~30% of Phox2b⁺cFos⁺ cells is necessary to produce impaired HCVR. Theoretically, a large fraction of Phox2b-expressing neurons must be eliminated to proportionally reduce CO₂-activated cells demanded for respiratory deficits. However, lesions of ~20% of Phox2b⁺ neurons have worked effectively in the

present experiment. The rational interpretation could be that Phox2b⁺cFos⁺ neurons are densely distributed in the medial, intermediate and dorsal subnuclei of the NTS, where the injections of SSP-SAP were made. This explanation is also reinforced by the findings of the present study suggesting that pH-sensitive Phox2b-expressing neurons were mainly located in the dorsal and medial parts of the NTS. Identifying the phenotype of CO₂-responsive neurons is of course valuable and has been used elsewhere to some advantage (RTN, raphe, etc.). We cannot completely rule out the possibility that the respiratory deficits caused by SSP-SAP are a result of the lesion of non-Phox2b-expressing neurons, although the use of Blank-SAP as a control reduces the argument. Blank-SAP

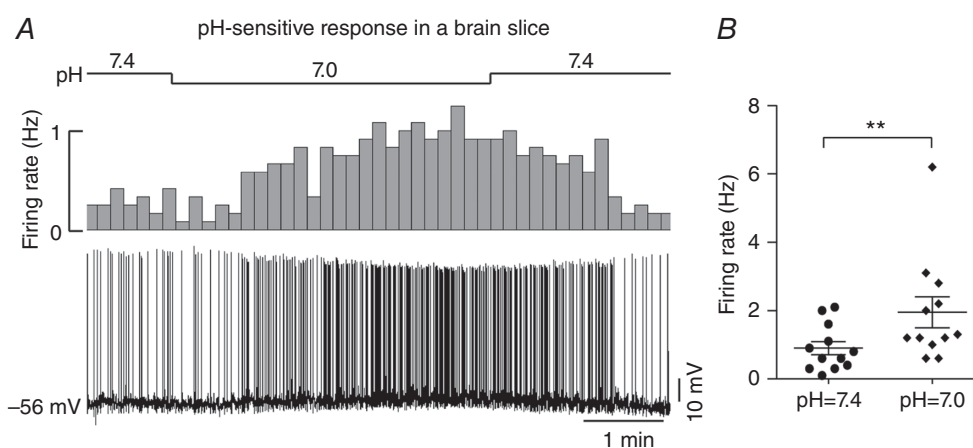


Figure 8. Effect of bath acidification on membrane potential and firing rate

A, typical whole-cell current clamp recordings of membrane potential and firing rate at differing bath pH in an EGFP-expressing neuron on a brainstem slice. Bath acidification depolarized membrane potential (~4 mV) and increased firing rate. B, average firing rate at bath pH 7.4 vs. 7.0. $n = 12$, $**P < 0.01$ by a two-tailed paired t test.

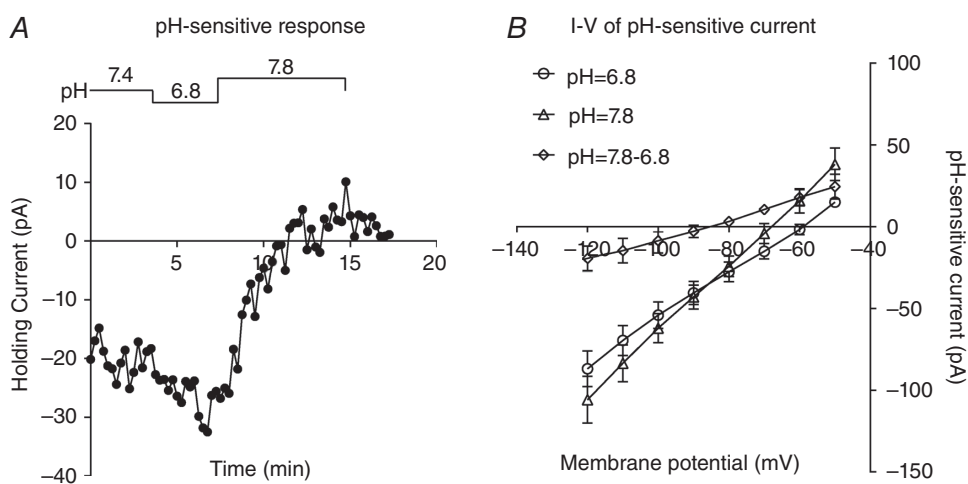


Figure 9. Effect of bath acidification on pH sensitive currents

A, whole-cell voltage clamp recordings obtained at different bath pH from an EGFP-expressing NTS neuron in a brainstem slice. Acidification decreases holding current and alkalization produces a reversible outward shift in holding current. B, average $I-V$ relationship of the pH-sensitive current (pH 7.8 to pH 6.8). Note that the reversible potential of pH-sensitive current is approximately -85 mV.

was without effect on ventilation, arguing against the possibility that the outcome is a result of mechanical damage caused by microinjection pipettes or surgical wound. Finally, most DMNV neurons were almost intact following microinjections of SSP-SAP, suggesting that the respiratory deficits are probably not a result of the loss of Phox2b-expressing DMNV neurons. Note that a decrease in MV could have multiple causes besides a reduction in chemosensitivity (e.g. trouble with lung feedback, vigilance issues, muscle fatigue, etc.), although the use of control and Blank-SAP-injected mice reduces such arguments. In summary, we suggest that the impairment of HCVR caused by injection of SSP-SAP is ascribed to the loss of CO₂-responsive Phox2b-expressing neurons.

Intrinsic chemosensitivity of Phox2b-expressing neurons

The chemosensitivity of NTS (or NTS-DMNV complex) neurons has been extensively studied in slices treated with blockers of synaptic transmissions and of gap junction, or in dissociated neurons (Dean & Putnam, 2010). The results of the present study obtained from acute slices and dissociated neurons clearly show that a subgroup of Phox2b-expressing NTS neurons (~43%) exhibits characteristic sensitivity to CO₂/H⁺, independent on synaptic transmission and paracrine signalling, providing solid evidence of an intrinsic pH sensitivity of these neurons. Nevertheless, we have no direct evidence linking the pH-sensitivity of the neurons recorded *in vitro* to the stimulatory effect of CO₂ on breathing.

Two issues concerning inherent pH sensitivity of NTS neurons remain to be addressed. The first one involves the mechanism underlying the molecular base sensing CO₂/H⁺ in the NTS. Early findings confirmed that 4-aminopyridine was able to completely eliminate the response of solitary complex neurons to hypercapnia, in support of contribution of a transient voltage-activated K⁺ channel in the chemosensitive response to acid challenges in the NTS (Dean *et al.* 1990). Consistent with prior report by Huda *et al.* (2012), we also demonstrate two patterned responses of Phox2b-expressing neurons to acidification challenge: transient and sustained. In addition, Huda *et al.* (2012) proposed that such transient responses to acidification were mediated by ASICs. Therefore, in the present study, we focused on revealing the ionic mechanism of sustained responses to acidification in Phox2b-expressing neurons. Our data implicate a background K⁺ channel in pH sensitivity of these neurons, although the subtype of such a K⁺ channel remains to be explored. In the RTN, G-protein coupled receptor 4 and/or Task-2 channels have been confirmed to contribute to neuronal pH sensitivity (Kumar *et al.* 2015), whereas the situation appears to be somewhat complicated according

to the above findings in the NTS. Although the ASICs and the background K⁺ channel function as molecular sensors in the NTS, we cannot exclude the involvement of other ionic mechanisms. Multiple pH-sensitive molecules or ion channels may work synergistically.

The second issue is related to molecular or genetic identification of pH-sensitive NTS neurons. The identity of the central respiratory chemoreceptors still remains controversial in part because chemosensitive cells have been widely distributed in the brainstem. The region-specific and cell type-specific phenotypes may account for the heterogeneity of these cells. Although great efforts have been made to determine the commonly biochemical phenotype of these cells, this remains poorly understood to date. In the RTN, > 90% Phox2b-expressing neurons are pH-sensitive, with concurrent immunoreactivity to vesicular glutamate transporter 2 (Lazarenko *et al.* 2009; Wang *et al.* 2013b). Selective stimulation or lesions of these RTN neurons affected central respiratory chemoreflex (Takakura *et al.* 2008; Abbott *et al.* 2009). Thus, Phox2b serves as a good molecular signature of the respiratory chemoreceptors in the RTN. In the present study, although ~74% of CO₂-activated NTS neurons were immunoreactive for Phox2b, ~10% of Phox2b⁺ neurons were CO₂-activated. Most probably, this is a result of the presence of a large number of Phox2b⁺ neurons in the NTS that are more heterogeneous than those in the RTN. At this point, Phox2b is not a specific marker of chemoreceptors in the NTS. Further work is required to identify the more specific molecular signature of central chemoreceptor neurons in this region.

Significance and summary

The mechanism of the respiratory deficits of CCHS remains incompletely understood to date. The respiratory symptoms of CCHS are the absence of HCVR and sleep-related central apnoeas (Weese-Mayer *et al.* 2010). Impaired HCVR has been closely associated with the structural and functional deficiency of Phox2b-expressing neurons, in particular, those neurons serving as central respiratory chemoreceptors (Guyenet & Bayliss, 2015). RTN neurons failed to develop in transgenic mice with mutated form of Phox2b and these mice displayed attenuated HCVR, suggesting a crucial role of Phox2b-expressing RTN neurons in the regulation of breathing (Dubreuil *et al.* 2009b). Besides, Nobuta *et al.* (2015) found that early-onset mutant Phox2b expression inhibited locus coeruleus neuronal development in a mouse model of CCHS, implying a potential impairment of regulation of breathing by the locus coeruleus. In the present study, elimination of Phox2b-expressing NTS neurons did not appear to contribute to basal breathing under normocapnic conditions but remarkably impaired HCVR. This makes sense, particularly under pathological

conditions, such as respiratory acidosis in obese hypoventilation syndrome or CCHS. It is therefore inferred that the respiratory deficits in Phox2b mutants may result from the loss of Phox2b-expressing neurons not only in the RTN, but also in the NTS. The present study extends the evidence of Phox2b-expressing neurons as candidate central chemoreceptors and provides new insights into clinical intervention targets.

Taken together, the blunted HCVR produced by injection of SSP-SAP is attributed to the proportional destruction of CO₂/H⁺-sensitive Phox2b-expressing NTS neurons, followed by the impaired excitatory drive to the respiratory pattern generator. The pH-sensitive Phox2b-expressing NTS neurons function as the central chemoreceptor responsible for the regulation of breathing. The results of the present study, combined with our previous data obtained in the RTN, can help us understand the mechanism of respiratory deficits in CCHS.

References

- Abbott SB, Stornetta RL, Fortuna MG, DePuy SD, West GH, Harris TE & Guyenet PG (2009). Photostimulation of retrotrapezoid nucleus phox2b-expressing neurons in vivo produces long-lasting activation of breathing in rats. *J Neurosci* **29**, 5806–5819.
- Berger AJ & Cooney KA (1982). Ventilatory effects of kainic acid injection of the ventrolateral solitary nucleus. *J Appl Physiol Respir Environ Exerc Physiol* **52**, 131–140.
- Cerpa V, Gonzalez A & Richerson GB (2014). Diphtheria toxin treatment of Pet-1-Cre floxed diphtheria toxin receptor mice disrupts thermoregulation without affecting respiratory chemoreception. *Neuroscience* **279**, 65–76.
- Dauger S, Pattyn A, Lofaso F, Gaultier C, Goridis C, Gallego J & Brunet JF (2003). Phox2b controls the development of peripheral chemoreceptors and afferent visceral pathways. *Development* **130**, 6635–6642.
- Dean JB, Bayliss DA, Erickson JT, Lawing WL & Millhorn DE (1990). Depolarization and stimulation of neurons in nucleus tractus solitarius by carbon dioxide does not require chemical synaptic input. *Neuroscience* **36**, 207–216.
- Dean JB, Kinkade EA & Putnam RW (2001). Cell-cell coupling in CO₂/H⁺-excited neurons in brainstem slices. *Respir Physiol* **129**, 83–100.
- Dean JB & Putnam RW (2010). The caudal solitary complex is a site of central CO₂ chemoreception and integration of multiple systems that regulate expired CO₂. *Respir Physiol Neurobiol* **173**, 274–287.
- Dubreuil V, Barhanin J, Goridis C & Brunet JF (2009a). Breathing with phox2b. *Philos Trans R Soc Lond B Biol Sci* **364**, 2477–2483.
- Dubreuil V, Thoby-Brisson M, Rallu M, Persson K, Pattyn A, Birchmeier C, Brunet JF, Fortin G & Goridis C (2009b). Defective respiratory rhythmogenesis and loss of central chemosensitivity in Phox2b mutants targeting retrotrapezoid nucleus neurons. *J Neurosci* **29**, 14836–14846.
- Gong S, Zheng C, Doughty ML, Losos K, Didkovsky N, Schambra UB, Nowak NJ, Joyner A, Leblanc G, Hatten ME & Heintz N (2003). A gene expression atlas of the central nervous system based on bacterial artificial chromosomes. *Nature* **425**, 917–925.
- Goridis C, Dubreuil V, Thoby-Brisson M, Fortin G & Brunet JF (2010). Phox2b, congenital central hypoventilation syndrome and the control of respiration. *Semin Cell Dev Biol* **21**, 814–822.
- Guyenet PG & Bayliss DA (2015). Neural control of breathing and CO₂ homeostasis. *Neuron* **87**, 946–961.
- Huda R, Pollema-Mays SL, Chang Z, Alheid GF, McCrimmon DR & Martina M (2012). Acid-sensing ion channels contribute to chemosensitivity of breathing-related neurons of the nucleus of the solitary tract. *J Physiol* **590**, 4761–4775.
- Kang BJ, Chang DA, Mackay DD, West GH, Moreira TS, Takakura AC, Gwilt JM, Guyenet PG & Stornetta RL (2007). Central nervous system distribution of the transcription factor Phox2b in the adult rat. *J Comp Neurol* **503**, 627–641.
- Kumar NN, Velic A, Soliz J, Shi Y, Li K, Wang S, Weaver JL, Sen J, Abbott SB, Lazarenko RM, Ludwig MG, Perez-Reyes E, Mohebbi N, Bettoni C, Gassmann M, Suply T, Seuwen K, Guyenet PG, Wagner CA & Bayliss DA (2015). Regulation of breathing by CO₂ requires the proton-activated receptor GPR4 in retrotrapezoid nucleus neurons. *Science* **348**, 1255–1260.
- Lazarenko RM, Milner TA, DePuy SD, Stornetta RL, West GH, Kievits JA, Bayliss DA & Guyenet PG (2009). Acid sensitivity and ultrastructure of the retrotrapezoid nucleus in Phox2b-EGFP transgenic mice. *J Comp Neurol* **517**, 69–86.
- Lin LH, Moore SA, Jones SY, McGlashon J & Talman WT (2013). Astrocytes in the rat nucleus tractus solitarius are critical for cardiovascular reflex control. *J Neurosci* **33**, 18608–18617.
- Lin LH, Nitschke DD & Talman WT (2012). Collateral damage and compensatory changes after injection of a toxin targeting neurons with the neurokinin-1 receptor in the nucleus tractus solitarius of rat. *J Chem Neuroanat* **43**, 141–148.
- Nattie E & Li A (2008). Muscimol dialysis into the caudal aspect of the Nucleus tractus solitarius of conscious rats inhibits chemoreception. *Respir Physiol Neurobiol* **164**, 394–400.
- Nattie EE & Li A (2002a). CO₂ dialysis in nucleus tractus solitarius region of rat increases ventilation in sleep and wakefulness. *J Appl Physiol* **92**, 2119–2130.
- Nattie EE & Li A (2002b). Substance P-saporin lesion of neurons with NK1 receptors in one chemoreceptor site in rats decreases ventilation and chemosensitivity. *J Physiol* **544**, 603–616.
- Nayate A, Moore SA, Weiss R, Taktakishvili OM, Lin LH & Talman WT (2009). Cardiac damage after lesions of the nucleus tractus solitarius. *Am J Physiol Regul Integr Comp Physiol* **296**, R272–R279.
- Nichols NL, Hartzler LK, Conrad SC, Dean JB & Putnam RW (2008). Intrinsic chemosensitivity of individual nucleus tractus solitarius (NTS) and locus coeruleus (LC) neurons from neonatal rats. *Adv Exp Med Biol* **605**, 348–352.

- Nobuta H, Cilio MR, Danhaive O, Tsai HH, Tupal S, Chang SM, Murnen A, Kreitzer F, Bravo V, Czeisler C, Gokozan HN, Gygli P, Bush S, Weese-Mayer DE, Conklin B, Yee SP, Huang EJ, Gray PA, Rowitch D & Otero JJ (2015). Dysregulation of locus coeruleus development in congenital central hypoventilation syndrome. *Acta Neuropathol* **130**, 171–183.
- Paxinos G & Franklin KBJ (2003). *The Mouse Brain in Stereotaxic Coordinates*. Academic Press, San Diego, CA.
- Stornetta RL, Moreira TS, Takakura AC, Kang BJ, Chang DA, West GH, Brunet JF, Mulkey DK, Bayliss DA & Guyenet PG (2006). Expression of Phox2b by brainstem neurons involved in chemosensory integration in the adult rat. *J Neurosci* **26**, 10305–10314.
- Takakura AC, Moreira TS, Stornetta RL, West GH, Gwilt JM & Guyenet PG (2008). Selective lesion of retrotrapezoid Phox2b-expressing neurons raises the apnoeic threshold in rats. *J Physiol* **586**, 2975–2991.
- Turovsky E, Theparambil SM, Kasymov V, Deitmer JW, Del Arroyo AG, Ackland GL, Corneveaux JJ, Allen AN, Huentelman MJ, Kasparov S, Marina N & Gourine AV (2016). Mechanisms of CO₂/H⁺ sensitivity of astrocytes. *J Neurosci* **36**, 10750–10758.
- Wang S, Benamer N, Zanella S, Kumar NN, Shi Y, Bevengut M, Penton D, Guyenet PG, Lesage F, Gestreau C, Barhanin J & Bayliss DA (2013a). TASK-2 channels contribute to pH sensitivity of retrotrapezoid nucleus chemoreceptor neurons. *J Neurosci* **33**, 16033–16044.
- Wang S, Shi Y, Shu S, Guyenet PG & Bayliss DA (2013b). Phox2b-expressing retrotrapezoid neurons are intrinsically responsive to H⁺ and CO₂. *J Neurosci* **33**, 7756–7761.
- Weese-Mayer DE, Berry-Kravis EM, Ceccherini I, Keens TG, Loghmanee DA & Trang H (2010). An official ATS clinical policy statement: congenital central hypoventilation syndrome: genetic basis, diagnosis, and management. *Am J Respir Crit Care Med* **181**, 626–644.
- Wiley RG & Kline IR (2000). Neuronal lesioning with axonally transported toxins. *J Neurosci Methods* **103**, 73–82.

Additional information

Competing interests

The authors have no competing interests to disclose.

Author contributions

CF, JX and SW conceived and designed the experiment. CF, JC, XW and LM performed the *in vivo* experiments. JX and RW performed the electrophysiological experiments. YZ and XZ co-ordinated the experiments. YL and FG analysed data. SW drafted the article. All authors revised the article critically for important intellectual content. All authors have approved the final version of the manuscript submitted for publication and agree to be accountable for all aspects of the work.

Funding

This work was supported by NNSF (31371166) and Hebei NSF (C2014206303).